The importance of along-margin terrane transport in northern Gondwana: insights from detrital zircon parentage in Neoproterozoic rocks from Iberia and Brittany

J. Fernández-Suárez[a;*], G. Gutiérrez Alonso[b], T.E. Jeffries[c]

[a] *Departamento de Petrología y Geoquímica Universidad Complutense, 28040 Madrid, Spain*
[b] *Departamento de Geología Universidad de Salamanca, 33708 Salamanca, Spain*
[c] *Department of Mineralogy, The Natural History Museum, London SW7 5BD, UK*

Abstract

Detrital zircons from late Neoproterozoic rocks of the peri-Gondwanan Cadomian belt of SW Iberia and north Armorican Domain of Brittany record Neoproterozoic (ca. 860-550 Ma), Palaeoproterozoic (ca. 2300-1800) and Archaean (ca 3300-2600 Ma) U-Pb ages. The absence of Mesoproterozoic zircons suggests that these terranes evolved in a peri-W African realm. This is in contrast to other western European terranes that preserve Mesoproterozoic zircons and are likely to have evolved in a peri-Amazonian realm. Such a contrast in detrital zircon populations, coupled with the presence of Mesoproterozoic zircons in the Ordovician Armorican quartzite, deposited in a peri- African platform, is interpreted to record along-margin terrane transport. The change in provenance suggests that subduction was replaced by transform faults that juxtaposed Amazonia-derived terranes against W Africa-derived terranes to form the Avalonia and Armorica microcontinents. Subsequent extension along the margin resulted in the birth of the Rheic Ocean and the outboard drift of Avalonia.

1. Introduction

Orogenic processes in active continental mar- gins involve major tectonic and thermal events leading to the creation, destruction and recycling of continental and oceanic crust, and the accretion, amalgamation and dispersal of crustal frag ments on different scales of space and time.

* Corresponding author. Tel.: +34-91-394-5013; Fax: +34-91-544-2535.
E-mail address: jfsuarez@geo.ucm.es (J. Fernández-Suárez).

Plate reorganisation at continental margins is often accompanied by substantial erosion and concomitant deposition of voluminous clastic sediments containing crucial information on the nature of the crustal elements in the provenance area.

The nature of plate processes and their importance in ancient orogens is commonly obscured by their involvement in subsequent tectonic events that destroy previous plate configurations. Overcoming this difficulty is particularly challenging in orogenic belts that have undergone more than one

episode of dispersal and accretion. This is the case for the Neoproterozoic Avalonian-Cadomian orogenic belt [1] that was dismembered in Cambro-Ordovician times with the opening of the Rheic Ocean. Subsequently, it became involved in the late Palaeozoic Variscan-Alleghanian orogeny, and finally, was dispersed again to its present-day arrangement in western Europe and eastern North America after the opening of the Atlantic Ocean.

Fundamental to our understanding and interpretation of these issues is the extent to which transform continental margins infiuence major crustal growth episodes and orogenic events [2]. Present-day tectonic settings such as the continental margin of western North America show the importance of along-margin terrane transport [2]. This has far-reaching implications for palaeo-geographic and plate reconstructions of ancient orogenic belts. In the case of early Palaeozoic and Precambrian orogenic belts, evidence for these processes is hard to find in the geological record. Even palaeomagnetic studies may fail to provide evidence for such processes as they may operate at scales of hundreds to a few thousands of km.

Nevertheless, valuable information concerning major tectonic events and former plate configurations, as well as constraints on the nature and age of basement source rocks, can be obtained by comparing U-Pb detrital zircon ages and/or Sm-Nd isotope signatures in coeval sedimentary rocks from separate terranes [3-10]. Here we use this approach to address first-order Neoproterozoic-early Palaeozoic tectonic events along the margin of north Gondwana taking key Cadomian-Avalonian terranes of the western European Variscan Belt as a case study.

1.1. Geology and palaeogeographic background

The late Palaeozoic Variscan collision belt of western Europe contains a mixture of crustal blocks with Neoproterozoic basement that origi- nally formed part of an assemblage of terranes along the peri-Gondwanan Cadomian-Avalonian arc [1,10]. It is generally agreed that these terranes formed as a result of Neoproterozoic subduction and arc construction along the northern Gond- wanan margin and that they were subsequently dispersed by the opening of the early Palaeozoic Rheic Ocean as subduction was replaced by transform/extensional activity [11,12]. Subsequent Palaeozoic plate tectonic motions that culminated in Appalachian-Variscan collisional orogenesis fur- ther redistributed these terranes toward their present arrangement in western Europe and Atlantic North Armorica. Reconstructing the tectonic evolution of these terranes and their location along the Cadomian-Avalonian orogen is fundamental to our understanding of major Neoproterozoic and early Palaeozoic tectonic events.

Palaeomagnetic studies, in addition to strati- graphic and palaeontological data, have provided a wealth of information on Neoproterozoic-early Palaeozoic continental reconstructions [13-15]. Yet, tighter constraints are needed in order to obtain a more detailed picture of the geography and tectonic setting of the northern Gondwanan margin and adjacent regions. Tracing the ancestry and evolution of the peri-Gondwanan terranes is further hindered by the absence of exposed pre-Neoproterozoic basement throughout most of the Cadomian-Avalonian Belt.

This study is focused on the Cadomian-Avalo- nian terranes presently exposed within the western European Variscan Belt (Fig. 1). Of particular interest are terranes such as Iberia and the Ar- morican Massif which feature major structural contacts between diferent tectonostratigraphic domains (Fig. 1). The origin and possible significance of these tectonic boundaries in the pre-Variscan evolution of these terranes are still poorly understood.

Restoration of the late Palaeozoic Iberian-Ar- morican Arc (Fig. 1) highlights the correlation of the Ossa Morena (SW Iberia) and the North American (Brittany) domains based on shared Neo- proterozoic-Lower Palaeozoic stratigraphy and abundance of igneous rocks formed during the time period ca 650-540 Ma [16]. Both domains record widespread Cadomian deformation and both are juxtaposed against the Central Iberian and South Armorican domains, respectively (Fig. 1). This juxtaposition occurs along major strike-slip faults with movement histories that

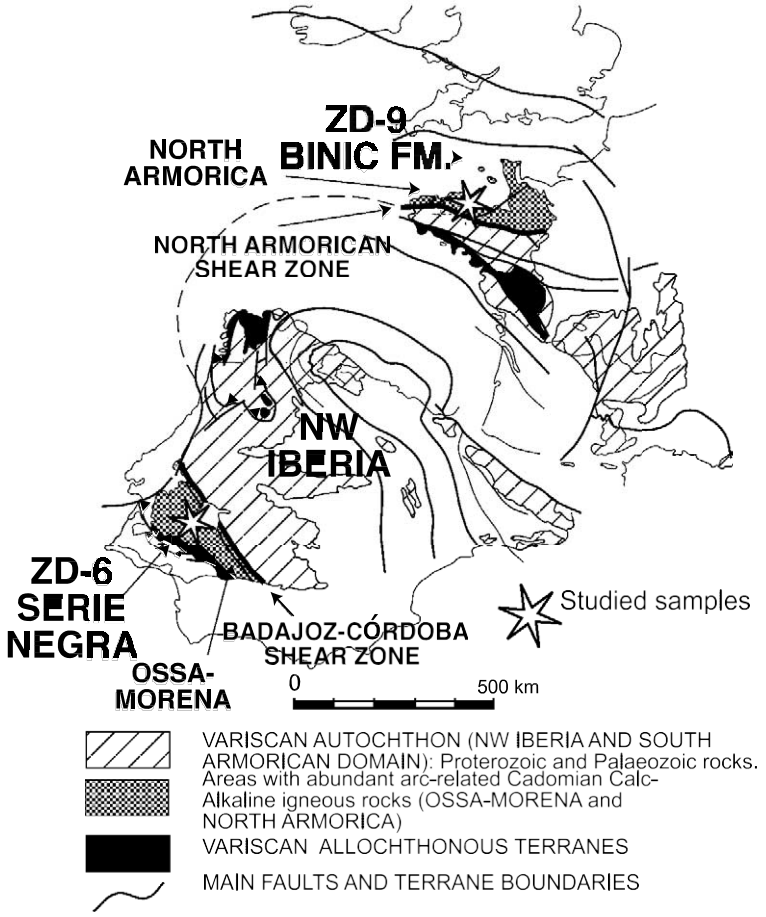

Fig. 1. Simplified geological map of Iberia and Cadomia showing location of samples ZD-6 (Ossa Morena, SW Spain) and ZD-9 (Brittany, NW France).

may predate the earliest recognised Variscan de- formation [16]. To test this correlation, two sam- ples were collected from low-grade greywackes in both domains (Fig. 1) in order to compare the age populations of their detrital zircons with those in the NW Iberian Domain [6,17]. Sample ZD-6 was collected in the Ossa Morena Zone (Province of Badajoz, SW Spain), in the upper part of the Serie Negra, in the core of the Olivenza-Monesterio antiform (Fig. 1). Sample ZD-9 was collected from Brioverian sediments of the Binic Forma- tion, north of the town of Binic (Brittany, NW France). Both formations are considered to be of late Neoproterozoic depositional age [18].

Sample ZD-6 is a coarse-grained heterometric lithic greywacke containing clasts of quartz, igneous rocks, micas and plagioclase in a matrix of fine-grained phyllosilicates with a coarse cleavage (pressure-solution seams). Sample ZD-9 is a medium-grained arkosic greywacke containing quartz, plagioclase and scarce igneous rock frag- ments in a matrix of recrystallised phyllosilicates that display a poorly developed cleavage.

2. U-Pb analytical methods

Mineral separation was performed at UCM (Madrid). The samples were crushed using a jaw crusher and pulverised with a disc mill. Heavy fraction enrichment on a Wilfley table, magnetic separation using a Frantz isodynamic separator

and density separation using di-iodomethane (CH_2I_2) were employed to separate the zircons. The zircons were hand-picked in alcohol under a binocular microscope and grains chosen to repre- sent all types found in the samples with regard to size, length-to-breadth ratio, roundness, colour, and other salient morphological features. Zircons selected for LA-ICP-MS analyses were set in syn- thetic resin (SpeciFix-201) mounts, polished to approximately half their thickness, and cleaned in a warm HNO_3 ultrasonic bath. Prior to analysis, cathodoluminiscence (CL) and backscattered electron (BSE) imaging was performed to ensure that analyses did not straddle diferent domains as indicated by the structure revealed by BSE and CL imaging.

U-Pb dating of individual zircon grains was performed using 213 nm laser ablation ICP-MS at The Natural History Museum (London). The 213 nm laser system had not been used previously to determine U-Pb isotopic ratios in zircons, and prior to its application to the unknown samples, the technique was validated and refined using zir- con standards and igneous zircons previously dated by IDTIMS. The main advantages of the 213 nm laser over the more widely used 266 nm laser are a slower, more stable ablation rate and the production of consistently small, readily trans- ported ablated particles. This results in increased signal stability and precision in the analyses. More detailed information on the features of ablation using a 213 nm laser is given in [19,20]. In view of the relatively large ablation pit size (typically 50-60 Wm), only zircons considered to be homogeneous on the basis of their CL/BSE images, or large cores, were analysed.

The instrumentation used consisted of a fre- quency quintupled Nd:YAG laser ablation sys- tem, V = 213 nm (New Wave Research, USA) coupled to a quadrupole based ICP-MS (Plasma- Quad 3, Thermo Elemental, UK) with an en- hanced sensitivity (S-option) interface. In this study, analyses were performed using argon as carrier gas. It is worth noting that a work in progress by the authors shows that the use of helium carrier gas greatly improves sample trans- port e/ciency, which reduces elemental fraction- ation and results in more concordant analyses. It has no efect on the precision of measured $^{207}Pb/^{206}Pb$ ratios.

To reduce the extent of inter-element laser-in- duced fractionation, the zircons were ablated at the lowest power density required to couple to the sample (pulse energy = 0.15 mJ per pulse). During ablation, the sample was moved relative to the beam along raster or line patterns, using a computer-controlled motorised stage.

Each analytical 'run' consisted of 20 analyses in the following order: four analyses of standard reference zircon 91500 [21], 12 analyses of the sample zircons and four analyses of standard 91500. After each analytical session, the raw data were downloaded to a PC for of-line pro- cessing. Raw count rates were integrated by aver- aging consecutive groups of 15 sweeps into single readings. The data were then processed using LAMTRACE, a data-reducing programme for la- ser ablation ICP-MS written by Simon E. Jack- son, Macquarie University, Sydney, Australia. Net background-corrected count rates for each isotope were used for calculation of sample ages. Age and error calculation are as described in [6,8] with two exceptions: (i) we use the standard reference zircon 91500 instead of the 02123 in-house standard, and (ii) we use measured $^{207}Pb/^{235}U$ ratios in our calculations. The data reported have internal precision (2c) based on counting statistics of each individual analysis.

For each determination, time-resolved signals were carefully studied to select stable, non-fractionated intervals, ensuring that inclusions, zona- tion or core-rim features were always excluded from age calculations.

3. Results

A total of 120 analyses were performed on sin- gle grains (one analysis per grain) from both sam- ples. Of these, 37 were rejected based on the cri- teria reported below. The results for selected analyses are given in Table 1 and presented as concordia diagrams and histograms in Figs. 2 and 3, respectively.

Although the analytical methodology (see above) ensures ablation of homogeneous zircon

Table 1
Laser ablation ICP-MS U-Pb analyses (concordant analyses in bold type)

Samp./Anal.#	Isotopic ratios (2c errors)			Age (Ma)			Best age estimate
	$^{206}Pb/^{238}U$	$^{207}Pb/^{235}U$	$^{207}Pb/^{206}Pb$	$^{206}Pb/^{238}U$	$^{207}Pb/^{235}U$	$^{207}Pb/^{206}Pb$	(Ma)
ZD-6							
Z1	0.0794 X 0.0004	0.6511 X 0.0036	0.0594 X 0.0002	493X4	509X4	582X16	582X16
Z2	0.0836 X 0.0006	0.6810 X 0.0057	0.0591 X 0.0003	518X8	527X7	568X22	568X22
Z3	0.0838 X 0.0007	0.6936 X 0.0044	0.0600 X 0.0003	519X8	535X5	602X24	602X24
Z4	0.0838 X 0.0005	0.7029 X 0.0063	0.0608 X 0.0004	519X6	541X7	632X30	632X30
Z5	0.0856 X 0.0005	0.7067 X 0.0048	0.0599 X 0.0003	529X6	543X6	598X20	598X20
Z6	0.0872 X 0.0005	0.7086 X 0.0047	0.0589 X 0.0003	540X6	544X6	564X22	564X22
Z7	0.0875 X 0.0005	0.7069 X 0.0060	0.0586 X 0.0005	541X5	543X7	550X20	541±3
Z8	0.0884 X 0.0007	0.7521 X 0.0064	0.0617 X 0.0003	546X8	569X7	662X20	662X20
Z9	0.0889 X 0.0008	0.7536 X 0.0068	0.0615 X 0.0002	549X9	570X8	654X16	654X16
Z10	0.0898 X 0.0007	0.7569 X 0.0066	0.0611 X 0.0004	554X8	572X8	642X30	642X30
Z11	0.0898 X 0.0004	0.7418 X 0.0034	0.0599 X 0.0003	554X5	563X4	600X20	600X20
Z12	0.0926 X 0.0007	0.7542 X 0.0067	0.0591 X 0.0004	571X9	571X8	568X28	571±4
Z13	0.0928 X 0.0008	0.7541 X 0.0075	0.0589 X 0.0003	572X9	571X9	562X22	571±4
Z14	0.0959 X 0.0010	0.7888 X 0.0077	0.0596 X 0.0006	591X12	591X9	588X42	591±5
Z15	0.0971 X 0.0007	0.7995 X 0.0065	0.0597 X 0.0003	597X8	597X7	592X20	597±4
Z16	0.0990 X 0.0012	0.8188 X 0.0094	0.0600 X 0.0004	609X14	607X11	600X32	607±5
Z17	0.1026 X 0.0006	0.8935 X 0.0072	0.0632 X 0.0003	629X7	648X8	714X22	714X22
Z18	0.1114 X 0.0013	0.9966 X 0.0175	0.0649 X 0.0010	681X15	702X18	768X64	768X64
Z19	0.1185 X 0.0007	1.1105 X 0.0077	0.0680 X 0.0002	722X8	758X7	866X12	866X12
Z20	0.1233 X 0.0007	1.1522 X 0.0075	0.0678 X 0.0003	749X8	778X7	860X18	860X18
Z21	0.2772 X 0.0033	4.3681 X 0.0590	0.1143 X 0.0005	1577X34	1706X22	1868X14	1868X14
Z22	0.2824 X 0.0020	4.6787 X 0.0426	0.1201 X 0.0005	1603X20	1763X15	1958X16	1958X16
Z23	0.2909 X 0.0025	4.6014 X 0.0428	0.1147 X 0.0004	1646X25	1750X15	1874X12	1874X12
Z24	0.2912 X 0.0019	4.6276 X 0.0305	0.1152 X 0.0004	1647X19	1754X11	1882X12	1882X12
Z25	0.3005 X 0.0028	5.3919 X 0.1202	0.1301 X 0.0026	1694X28	1884X38	2098X68	2098X68
Z26	0.3025 X 0.0018	5.0316 X 0.0327	0.1206 X 0.0007	1704X17	1825X11	1964X22	1964X22
Z27	0.3068 X 0.0018	5.3052 X 0.0355	0.1254 X 0.0003	1725X18	1870X11	2034X8	2034X8
Z28	0.3104 X 0.0026	4.9953 X 0.0495	0.1167 X 0.0007	1743X25	1819X17	1906X22	1906X22
Z29	0.3159 X 0.0027	5.3759 X 0.0430	0.1234 X 0.0003	1770X27	1881X14	2004X10	2004X10
Z30	0.3180 X 0.0022	5.8373 X 0.0946	0.1331 X 0.0018	1780X21	1952X28	2138X48	2138X48
Z31	0.3342 X 0.0021	5.2517 X 0.0373	0.1140 X 0.0003	1859X21	1861X12	1862X10	1862±6
Z32	0.3485 X 0.0070	5.5957 X 0.1158	0.1165 X 0.0003	1927X67	1915X36	1902X10	1902±8
Z33	0.3487 X 0.0040	5.9122 X 0.0656	0.1229 X 0.0005	1929X38	1963X19	1998X14	1998X14
Z34	0.3642 X 0.0034	6.5804 X 0.0691	0.1310 X 0.0006	2002X32	2057X19	2110X16	2110X16
Z35	0.3829 X 0.0021	7.0189 X 0.0316	0.1329 X 0.0007	2090X20	2114X8	2136X16	2136X16
Z36	0.4043 X 0.0033	8.4528 X 0.0718	0.1516 X 0.0004	2189X30	2281X15	2364X10	2364X10
Z37	0.4513 X 0.0039	11.0716 X 0.1163	0.1779 X 0.0006	2401X35	2529X20	2632X12	2632X12
Z38	0.4582 X 0.0049	11.5137 X 0.1267	0.1822 X 0.0005	2431X43	2566X21	2672X8	2672X8
Z39	0.5168 X 0.0041	16.2267 X 0.1314	0.2277 X 0.0004	2685X35	2890X15	3034X6	3034X6
Z40	0.5369 X 0.0029	16.9163 X 0.0998	0.2285 X 0.0005	2771X24	2930X11	3040X6	3040X6
Z41	0.5726 X 0.0043	21.3067 X 0.1385	0.2698 X 0.0013	2919X35	3153X13	3304X16	3304X16
Z42	0.6207 X 0.0036	22.9077 X 0.1489	0.2676 X 0.0014	3113X29	3223X13	3292X16	3292X16
ZD-9							
Z43	0.0904 X 0.0007	0.7320 X 0.0053	0.0587 X 0.0002	558X8	558X6	556X12	558±4
Z44	0.0894 X 0.0005	0.7324 X 0.0050	0.0594 X 0.0003	552X6	558X6	580X22	580X22
Z45	0.0874 X 0.0007	0.7221 X 0.0061	0.0599 X 0.0004	540X8	552X7	598X30	598X30
Z46	0.0898 X 0.0006	0.7466 X 0.0051	0.0603 X 0.0002	555X7	566X6	612X12	612X12
Z47	0.0886 X 0.0005	0.7389 X 0.0044	0.0605 X 0.0002	547X5	562X5	620X18	620X18
Z48	0.0878 X 0.0008	0.7320 X 0.0072	0.0605 X 0.0003	543X9	558X8	620X18	620X18
Z49	0.0904 X 0.0008	0.7573 X 0.0064	0.0607 X 0.0002	558X9	572X7	630X18	630X18
Z50	0.0863 X 0.0006	0.7234 X 0.0072	0.0608 X 0.0004	533X7	553X8	632X26	632X26

Table 1 (*Continued*).

Samp./Anal.#	Isotopic ratios (2c errors)			Age (Ma)			Best age estimate
	$^{206}Pb/^{238}U$	$^{207}Pb/^{235}U$	$^{207}Pb/^{206}Pb$	$^{206}Pb/^{238}U$	$^{207}Pb/^{235}U$	$^{207}Pb/^{206}Pb$	(Ma)
Z51	0.0934 X 0.0005	0.7849 X 0.0050	0.0610 X 0.0003	576X5	588X6	636X24	636X24
Z52	0.0974 X 0.0009	0.8219 X 0.0081	0.0612 X 0.0001	599X11	609X9	646X10	646X10
Z53	0.0867 X 0.0008	0.7315 X 0.0068	0.0612 X 0.0003	536X9	557X8	646X18	646X18
Z54	0.0915 X 0.0013	0.7754 X 0.0118	0.0614 X 0.0004	565X15	583X13	654X32	654X32
Z55	0.0898 X 0.0009	0.7633 X 0.0082	0.0616 X 0.0006	554X11	576X10	660X40	660X40
Z56	0.0917 X 0.0009	0.7816 X 0.0098	0.0618 X 0.0003	566X11	586X11	666X18	666X18
Z57	0.0895 X 0.0006	0.7627 X 0.0044	0.0618 X 0.0002	552X7	576X5	666X16	666X16
Z58	0.0924 X 0.0008	0.7885 X 0.0078	0.0619 X 0.0004	569X9	590X9	670X24	670X24
Z59	0.1183 X 0.0012	1.0132 X 0.0105	0.0621 X 0.0003	721X14	711X11	676X22	676X22
Z60	0.0980 X 0.0008	0.8409 X 0.0071	0.0622 X 0.0003	603X9	620X8	682X22	682X22
Z61	0.0897 X 0.0007	0.7712 X 0.0079	0.0624 X 0.0006	554X9	580X9	686X44	686X44
Z62	0.1012 X 0.0008	0.8825 X 0.0072	0.0632 X 0.0004	622X10	642X8	714X28	714X28
Z63	0.1031 X 0.0008	0.9042 X 0.0093	0.0636 X 0.0004	632X9	654X10	728X24	728X24
Z64	0.1092 X 0.0005	0.9851 X 0.0126	0.0654 X 0.0006	668X6	696X13	786X40	786X40
Z65	0.1115 X 0.0007	1.0195 X 0.0076	0.0663 X 0.0003	681X8	714X8	814X22	814X22
Z66	0.1299 X 0.0008	1.1972 X 0.0104	0.0669 X 0.0006	787X9	799X10	832X38	832X38
Z67	0.1397 X 0.0010	1.2926 X 0.0103	0.0671 X 0.0005	843X12	842X9	840X32	843±5
Z68	0.2842 X 0.0027	4.7056 X 0.0391	0.1200 X 0.0004	1613X28	1768X14	1956X12	1956X12
Z69	0.3123 X 0.0013	5.2156 X 0.0235	0.1211 X 0.0004	1752X13	1855X8	1972X10	1972X10
Z70	0.3391 X 0.0013	5.8282 X 0.0303	0.1246 X 0.0003	1882X12	1951X9	2022X10	2022X10
Z71	0.2954 X 0.0020	5.1531 X 0.0392	0.1265 X 0.0002	1669X20	1845X13	2048X6	2048X6
Z72	0.2949 X 0.0021	5.2888 X 0.0439	0.1300 X 0.0005	1666X21	1867X14	2098X14	2098X14
Z73	0.3464 X 0.0055	6.5536 X 0.1167	0.1372 X 0.0024	1917X53	2053X31	2190X62	2190X62
Z74	0.3710 X 0.0029	7.1334 X 0.0578	0.1395 X 0.0002	2034X27	2128X14	2220X6	2220X6
Z75	0.4170 X 0.0025	8.3922 X 0.0814	0.1460 X 0.0010	2247X23	2274X18	2298X24	2298X24
Z76	0.3812 X 0.0032	7.7401 X 0.0418	0.1473 X 0.0007	2082X30	2201X10	2314X18	2314X18
Z77	0.5333 X 0.0077	12.4708 X 0.1796	0.1696 X 0.0007	2755X64	2641X27	2552X14	2552X14
Z78	0.4551 X 0.0090	11.0839 X 0.2250	0.1766 X 0.0011	2418X80	2530X38	2620X22	2620X22
Z79	0.4536 X 0.0020	11.2347 X 0.0528	0.1796 X 0.0005	2411X18	2543X9	2648X8	2648X8
Z80	0.5299 X 0.0039	13.4333 X 0.0994	0.1839 X 0.0009	2741X33	2711X14	2686X16	2686X16
Z81	0.5418 X 0.0046	14.5080 X 0.1190	0.1942 X 0.0004	2791X38	2784X16	2776X6	2779±4
Z82	0.5936 X 0.0045	19.7721 X 0.1186	0.2416 X 0.0012	3004X36	3080X12	3130X16	3130X16
Z83	0.7534 X 0.0052	28.8080 X 0.1815	0.2773 X 0.0006	3620X38	3447X12	3346X6	3346X6

domains, analyses with ≤ 20% discordance (calculated from $[^{206}Pb/^{238}U]/[^{207}Pb/^{206}Pb]$ age) were rejected. The time-resolved analysis software re- ports signal intensity (counts per second) for every mass sweep performed by the mass spec- trometer. This protocol, allowing acquisition of signals as a function of time (a proxy for ablation depth profile), permits the recognition of isotopic heterogeneity and therefore the detection of inclusions, high common Pb associated to fractures or areas of radiation damage, and inherited Pb components (older cores). All analyses whose time-resolved signals showed any suspect features were excluded from the data set irrespective of their discordance. Using this approach, it can be assumed confidently that discordance in the selected analyses is not due to mixing of diferently aged zircon domains but by lead loss and perhaps mi- nor U-Pb laser-induced elemental fractionation, undetectable in the time-resolved signals. Such fractionation does not afect the measured $^{207}Pb/^{206}Pb$ ratios.

The ages reported in this paper are not common Pb-corrected as ^{204}Pb measurements are ren- dered useless by the isobaric interference from Hg, a contaminant present in the argon supply gas. ^{204}Hg interferes on ^{204}Pb and the ^{202}Hg peak is commonly too small to allow a reliable overlap correction of acceptable precision [22].

Since the LA-(quadrupole)-ICP-MS technique

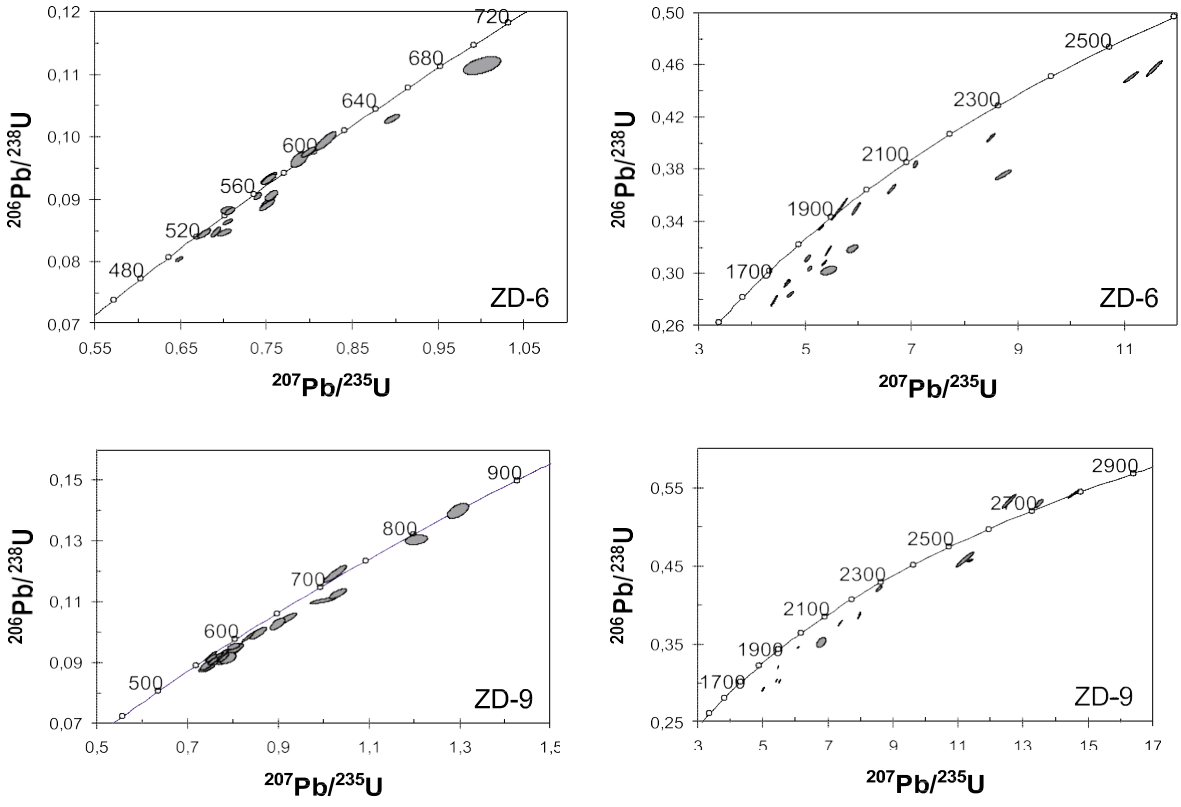

Fig. 2. Concordia plots of U-Pb analytical data from samples ZD-6 and ZD-9. Ellipses represent 2c uncertainties.

using a natural zircon standard does not allow reliable determination of ^{204}Pb, an alternative op- tion would be to use the ^{208}Pb correction [23]. However, this method can only be applied if the $ThO^{þ}/UO^{þ}$ ratio [23] can be simultaneously determined with acceptable precision or assuming concordance of $^{206}Pb/^{238}U$ and $^{208}Pb/^{232}Th$ ages. As the assumption cannot be justified a priori, it is felt that this correction method should not be applied to analyses such as those reported in this study (cf. [24]). The $^{208}Pb/^{232}Th$ ratio (not reported in Table 1) is very sensitive to common Pb contamination, resulting in $^{208}Pb/^{232}Th$ ages that are significantly older than the $^{206}Pb/^{238}U$ ages. This feature ofers a qualitative criterion to detect zircons with high common Pb content in LA-ICP-MS analyses [9]. In this study we found this feature only in analyses where $^{206}Pb/^{238}U$- $^{207}Pb/^{206}Pb$ discordance is ≤ 20% and therefore would have been rejected irrespective of this fact.

Furthermore, it should be emphasised that most zircons do not contain significant amounts of common Pb and that for most Proterozoic zircons, common Pb corrections would be within the analytical uncertainty of the analyses reported here. For example, a SHRIMP study of zircons from a Neoproterozoic sedimentary formation of SW Iberia (stratigraphically equivalent to that in which sample ZD-6 was collected) [25] shows that the percentage of common ^{206}Pb relative to total measured ^{206}Pb is less than 0.5% in 80% of the analyses and ≤ 1% in only 10% of the analyses reported. In [25] all analyses with significant amounts of common Pb are ≤ 25% discordant (usually with reverse discordance) and have high Th contents. Finally, it should be noted that the age clusters derived from common Pb-corrected U-Pb data in [25] coincide with those reported in this study for a formation of stratigraphic equivalence (see below).

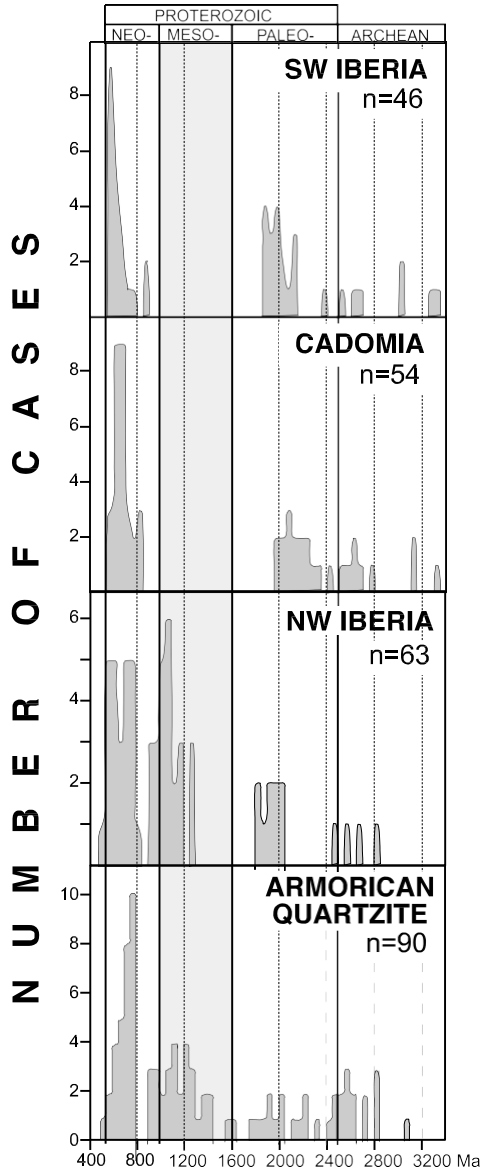

Fig. 3. Histograms of U-Pb ages for analysed samples from Ossa Morena Zone, SW Iberia (ZD-6) and north Armorican Domain (ZD-9) compared to previously analysed samples from NW Iberia [6] and the Armorican quartzite [17].

Considering the above arguments, we are confident that, in the carefully screened analyses reported here, only a very small percentage of the discordant $^{207}Pb/^{206}Pb$ ages might be slightly older than the 'correct age'. As the purpose of this study is to define age clusters in detrital zircon populations representing major crust formation events, the possible uncertainty associated with some of the discordant ages is insignificant to the interpretation of the data and has no influence on the main conclusions reached in this study. As a routine further precaution, those discordant analyses whose $^{207}Pb/^{206}Pb$ ages have no concordant counterparts are not used to derive geological conclusions, i.e. we only consider conclusions that would not be afected if solely $^{207}Pb/^{206}Pb$ or $^{206}Pb/^{238}U$ ages were used. As is the case in this study, the reliability of detrital zircon LA-ICP- MS U-Pb data is strengthened by the reproduc- ibility of age patterns in samples that are considered equivalent on the basis of independent geological criteria [6].

In the data presented here, a few data points plot slightly above concordia (Fig. 2; i.e. the $^{207}Pb/^{206}Pb$ age is younger than the $^{206}Pb/^{238}U$ and $^{207}Pb/^{235}U$ ages). This phenomenon of reverse discordance is frequently observed in both SIMS and LA-ICP-MS U-Pb analyses and although not well understood, it is generally attributed to redis- tribution of radiogenic lead on a micron scale [24,26] or associated with poor correction for U-Pb fractionation (fractionation in the sample deviates significantly from that in the standard) [8]. In either case, the $^{207}Pb/^{206}Pb$ ratio gives the best age estimate as the efect is comparable to moving the point up or down a discordia line going through 0 Ma (assuming that no other sources for discordance play a significant role).

The ages reported in the histograms of Fig. 3 and labelled 'best age estimate' in Table 1 are obtained as follows: For concordant analyses (ages whose corresponding isotope ratios have a 2c error ellipse that, to a greater or lesser extent, overlaps the concordia curve) we use concordia ages and errors as defined by Ludwig [27]. For discordant analyses we use the $^{207}Pb/^{206}Pb$ ages and 2c errors.

If we assume that discordant analyses can be attributed to Pb loss and since the efect of pos- sible episodic lead loss at intermediate ages can- not be evaluated, individual $^{207}Pb/^{206}Pb$ dates rep- resent minimum ages of growth for a given zircon. Again, as in these types of studies the clustering of grain ages is the crucial indicator of zircon-

forming high-grade events and since the efect of Pb loss is to disperse zircon ages [4] (i.e. broad- ening the spectra), the presence of well-defined clusters must be considered geologically significant.

The U-Pb ages in sample ZD-6 (Ossa Morena Zone, SW Iberia) show a predominance of zircons in the range 540-860 Ma (Figs. 2A and 3). The youngest zircon has a $^{206}Pb/^{238}U$ age of 541 X 6 Ma (concordia age of 541.4 X 2.4 Ma) and a less precise $^{207}Pb/^{206}Pb$ age of 550 X 20 Ma (2c). Con- cordant zircon ages in this cluster spread between ca 541 and 608 Ma, whereas discordant ages (6 20% discordance) spread from ca 560 to 866 Ma. Of these discordant analyses (Table 1) seven fall within the range of concordant analyses and eight have older $^{207}Pb/^{206}Pb$ ages from 632 to 866 Ma. Although no concordant zircons in this older range were dated in this study, Ordo nez Casado [25] reported common Pb-corrected SHRIMP ages for zircons in a stratigraphically equivalent formation spanning 541X19 to 847X26 Ma.

The second zircon cluster is of Palaeoprotero- zoic age (ca 1860-2300 Ma; Table 1). The young- est zircon in this group is sub-concordant (2.2% discordance) with a $^{207}Pb/^{206}Pb$ age of 1860 X 10 Ma. 15 zircons have ages ranging from ca 1860 to 2130 Ma (Table 1, Figs. 2B and 3). One zircon yielded an older discordant $^{207}Pb/^{206}Pb$ age of 2364 X 10 Ma. Five zircons yielded $^{207}Pb/^{206}Pb$ Archaean ages in the range ca 2600-3300 Ma (Fig. 3) with discordance 6 12%.

Zircon U-Pb ages in sample ZD-9 (Brittany) show a pattern similar to that of ZD-6 (Table 1, Figs. 2C,D and 3). The youngest age cluster is of Neoproterozoic age, ca 550-840 Ma. The young- est zircon in this group is concordant (30.4% dis- cordance) with a $^{206}Pb/^{238}U$ age of 558 X 8 Ma, within analytical error of the $^{207}Pb/^{206}Pb$ age of the youngest zircon in sample ZD-6. The oldest zircon in this cluster has a concordia age of 843 X 5 with 85% probability of concordance, very similar to the $^{207}Pb/^{206}Pb$ age of the oldest zircon of this group in sample ZD-6 (866X12 Ma).

The second most abundant group consists of Palaeoproterozoic zircons with ages ranging from ca 1950 to 2300 Ma (Table 1, Figs. 2D and 3). As in SW Iberia, a few zircons yielded Archaean ages (2550-3350 Ma). Each of these age groups is consistent with U-Pb IDTIMS sin gle-grain data from detrital zircons in the stratigraphically equivalent Jersey Shale Formation [28].

4. Discussion

4.1. Significance of U-Pb ages

The ages of the youngest detrital zircons in both formations are equivalent within analytical uncertainty, suggesting a coeval maximum late Neoproterozoic depositional age. These data are in agreement with other studies [18] and support their stratigraphic equivalence. This is an important constraint when interpreting detrital zircon ages, particularly at active continental margins like the Cadomian-Avalonian orogen, where pa- laeogeographic settings and source area exposures can vary significantly in short time intervals.

The similar U-Pb age populations of the detrital zircons in late Neoproterozoic greywackes from SW Iberia and the North Armorican Domain both indicate provenance from a crustal source formed shortly before deposition and older cratonic sources. Those Neoproterozoic ages in the range ca 540-560 to 620-650 Ma match the span of the main episodes of magmatic activity related to subduction and arc construction along the northern Gondwanan margin (compilation in [29]). Zircons with Neoproterozoic ages older than ca 650 Ma could have been generated either during the early arc phase [6,11] or they could represent detritus from rocks generated in Neoproterozoic interior orogens related to the assembly of west Gondwana [30,31].

Palaeoproterozoic zircon ages match the spread of loosely constrained orogenic events recorded in the west African craton [32] and Amazonia [33,34]. The presence of these zircons in the studied rocks is in agreement with the existence of a Palaeoproterozoic (ca 1.8-2.1 Ga) basement in western Europe (Icartian basement) [35,36]. Ar- chaean zircons dated in this study match the age spread of orogenic events recorded in cratonic

areas of west Africa [37-39] and Amazonia [34,40]. Therefore, the U-Pb age clusters found in the studied rocks indicate a clear Gondwanan signature for these late Neoproterozoic sedimentary formations.

4.2. Geodynamic implications

The Cadomian-Avalonian terranes of western Europe and Atlantic North America were devel- oped upon, and recycled material from, a cratonic basement whose age and composition varied along the northern Gondwanan margin [1]. With the exception of the ca 2 Ga Icartian gneisses in Brittany and the Channel Islands [35,36], this basement is not exposed and insights into its age and composition must be gained indirectly through U-Pb and Sm-Nd isotopic studies of Neoproterozoic and early Palaeozoic rocks. Such studies have identified two main basement signatures; one with affinities to west Africa and the other with affinities to Amazonia. Characteristic of the latter is the presence of Mesoproterozoic zircons (1600-1000 Ma), coupled generally with higher initial ε_{Nd} values (e.g. [1]).

The most significant feature of the detrital zircon ages from SW Iberia and Brittany is therefore the absence of Mesoproterozoic zircons. This contrasts with Neoproterozoic and early Palaeozoic sedimentary rocks in NW Iberia (Fig. 3) and other areas of the Central European Variscides (West Sudetes and Erzgebirge [41] and Moravo-Silesian Zone [42]), and with those reported from West Avalonia [1,5,29].

The lack of Mesoproterozoic (Grenvillian, Sun- sas-Rondonian) detrital zircons suggests that the SW Iberian and north Armorican fragments of the Cadomian-Avalonian orogen like most of the Saxothuringian and Moldanubian zones of central Europe which show similar detrital age characteristics [43,44] occupied a realm that had no access to exposures of basement rocks contain- ing Mesoproterozoic zircons. Of the likely craton- ic provenances, only the west African craton lacks significant zircon-forming Mesoproterozoic events, suggesting that SW Iberia, the north Armorican Domain and parts of the Bohemian Massif prob- ably lay adjacent to this craton at that time (Fig. 4A). NW Iberia, NE Bohemia and Moravo-Silesia, on the other hand, require a Mesoproterozoic basement source, suggesting closer proximity to Amazonia or Oaxaquia [45] (Fig. 4A).

The contrast in sedimentary provenance be- tween west Africa and Amazonia is also reflected in Sm-Nd isotope signatures. Rocks with west African affinities show much lower initial ε_{Nd} val- ues than those with Amazonian affinity. For ex- ample, the Neoproterozoic greywackes from NW Iberia record initial ε_{Nd} values between 0 and 35 [46], whereas greywackes of equivalent age in SW Iberia record initial ε_{Nd} values between 39 and 312 [47].

All these terranes formed part of the active northern margin of Gondwana (Fig. 4A) that featured both a magmatic arc and a variety of back- arc basins (e.g. [11]). A back-arc setting has been proposed for both NW Iberia [6] and NE Bohemia [41]. These regions may have been closer to the Gondwanan margin than the West Avalonian terranes, which are dominated by magmatic arc rocks and likely represent the main magmatic ed- ifice on the Amazonian segment of the margin (Fig. 4A).

Subduction along the margin proceeded until either ridge-trench collision [11] or a change in subduction regime [6] caused progressive transition to a transform regime (Fig. 4B-D). The arrest of subduction is considered to have been diachronous along the margin (e.g. [11] and references therein). This is consistent with the contrasting evolution of SW Iberia and Brittany with respect to NW Iberia and the predominance of younger Neoproterozoic detrital zircons in rocks from Brittany and SW Iberia in relation to those from NW Iberia (Fig. 3).

In the western European Variscan Belt, terranes with difering (Amazonian versus west African) basement signatures were juxtaposed prior to the deposition of the Middle Ordovician Armorican quartzite [48], which oversteps the boundaries be- tween these domains. This is the case of NW and SW Iberia (Fig. 1), the Armorican Massif and the diferent domains that make up the Bohemian Massif, and implies that crustal units separated by hundreds or thousands of km in the Neopro- terozoic had been amalgamated before Middle

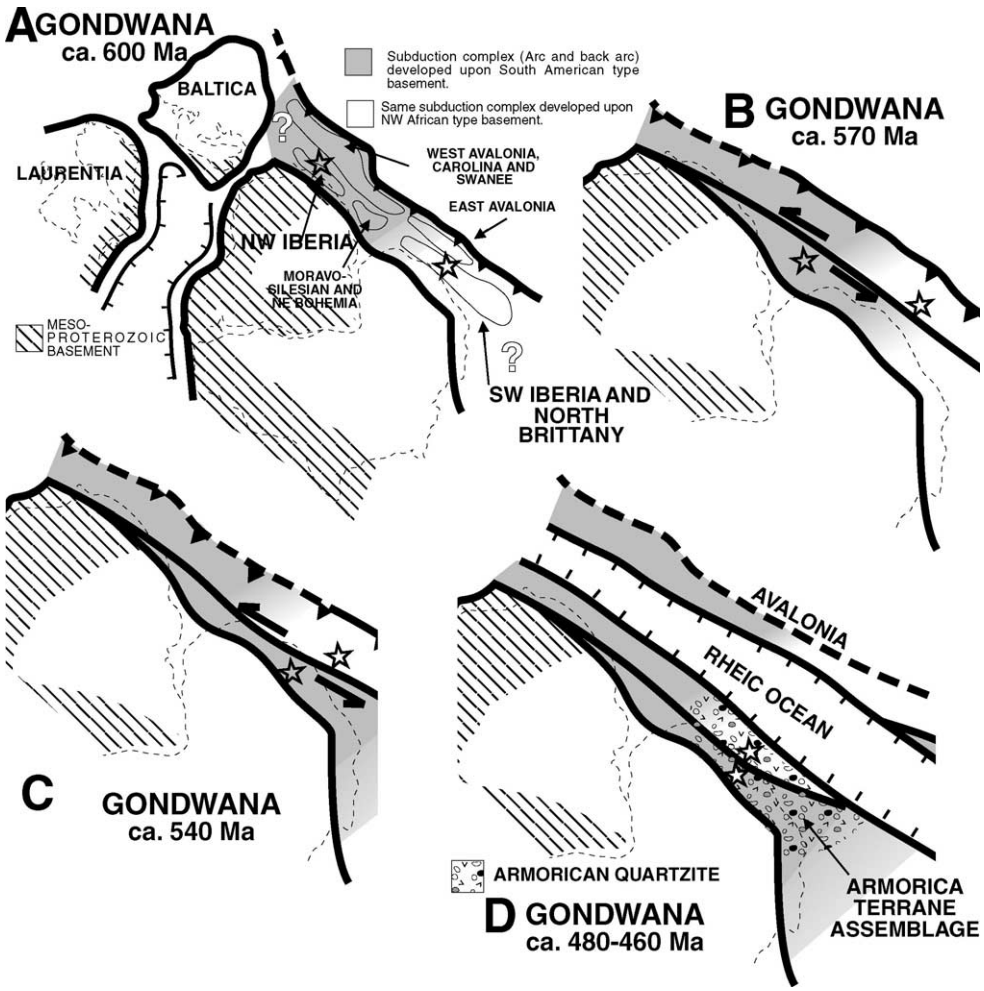

Fig. 4. Proposed Neoproterozoic terrane distribution (A,B) and early Palaeozoic tectonic evolution (C,D) along the northern Gondwanan margin (see text for details). Stars represent the hypothetical location of NW Iberia and SW Iberia/Brittany. Fig. 4A modified after [1] and [6].

Ordovician times. This amalgamation is sup- ported by faunal, palaeomagnetic and geologic evidence which all indicate that NW and SW Iberia, the Armorican Massif and Bohemia had all been assembled adjacent to west Africa to form the Armorican realm (or Armorican Terrane Assemblage) by the Early to Middle Ordovician ([14] and references therein).

If the Armorican quartzite was deposited upon an extensive peri-African continental platform [48,49], then the abundance of Mesoproterozoic zircons in this formation in NW Iberia [17] (Fig. 3) suggests that the source for these zircons had been tectonically transferred from an Amazonian realm before the deposition of the quartzite.

Therefore we propose that, prior to the Ordo- vician, NW Iberia (and other peri-Amazonian terranes of the Armorican Terrane Assemblage) were translated along the Gondwanan margin from an Amazonian realm towards the margin of west Africa. Later erosion of these tectonically trans- ported crustal fragments produced detritus containing Mesoproterozoic zircons that was incorporated into the Armorican quartzite.

Further, we suggest that this dispersal took place along major transform faults roughly paral-

lel to the Gondwanan margin (Fig. 4) and pro- ceeded until the peri-Amazonian terranes had docked against those that had occupied a peri- west African location since the Neoproterozoic (Fig. 4C). This would explain why peri-Gond- wanan terranes with difering basement signatures are presently juxtaposed in the western European Variscan Belt.

This tectonic amalgamation gave birth to the Armorica Terrane Assemblage, which evolved as a single unit until its involvement in the Variscan- Appalachian collision in the late Palaeozoic. Geo- logical evidence for this docking may be recorded at the tectonic contact between the NW and the SW Iberian terranes [16,50] (Fig. 1), which we interpret as a reactivated early Palaeozoic terrane boundary. Deposition of the Armorican quartzite at ca 465 Ma [51] provides a minimum age constraint for the docking between west Africa and Amazonia-derived terranes.

Shortly following (and/or partially overlapping) this dispersal of terranes along the Gondwanan margin a change in tectonic regime gave rise to extension on the margin and the birth of the Rheic Ocean. Rifting occurred between Armorica (an inboard terrane assemblage) and the more outboard Avalonia (Fig. 4D), which progressively separated from Gondwana until its docking to Laurentia-Baltica in the Silurian.

4.3. Further remarks

Margin-parallel strike-slip motion of terranes, as proposed here for north Gondwana, is observed in modern settings like the Cordilleran margin of North America [2] but has seldom been documented at this scale in ancient orogenic belts. We speculate that the peri-Gondwanan terranes with Amazonian affinities moved towards the west African margin in a manner akin to that in which California (west of the St. Andreas fault) is moving towards Alaska. The west African margin, in which subduction may still have been active when the strike-slip motion was initiated on the Amazonian side [11], could have acted as a back-stop to Africa-wards drifting terranes. Thus the Armorica Terrane Assemblage could be regarded as a bundling of terranes generated by strike-slip motion along the northern Gondwanan margin.

5. Conclusions

Detrital zircon ages in Neoproterozoic and early Palaeozoic sedimentary rocks from western Europe provide a record of the geography and geodynamic evolution along the northern Gond- wanan margin from ca 600 to 480 Ma. Such studies can provide first-order constraints on the histories of terrane dispersal and accretion, particularly in those cases where the geological record has been obscured by major orogenic events or subsequent plate reorganisation.

Constraining these processes in ancient orogenic belts can significantly improve our understanding of the geological record. We have demonstrated that U-Pb geochronology of detrital zircon populations can be used to test the role of transform margins in ancient orogens and crus- tal growth episodes.

Acknowledgements

This study was funded through an EU SYS-Resource (TMR Program) grant to J.F.S. J.F.S. also acknowledges a ‘Contrato de Reincorporación para Doctores y Tecnólogos’ from the Spanish Ministry of Education. Additional funding to G.G.A. was provided by Project BTE2000-1490- C02-01 of the Spanish Ministry of Education. The Electron Microscopy and Mineral Analysis Division, Frances Wall, and Lyanne Houseago (NHM) are kindly acknowledged for technical and logistic support. A. Azor and I. Expósito are thanked for useful sampling advise. Brendan Murphy, Sue Keay and an anonymous reviewer are kindly acknowledged for very insightful and constructive reviews. This paper is a contribution to IGCP Project 453.*[BARD]*

References

[1] R.D. Nance, J.B. Murphy, Contrasting basement signtures and the palinspastic restoration of peripheral oro- gens: an example from the Neoproterozoic Avalonian Cadomian Belt, Geology 22 (1994) 617-620.

[2] P.J. Pacthett, C.G. Chase, Role of transform continental margins in major crustal growth episodes, Geology 30 (2002) 39-42.

[3] G.E. Gehrels, G.M. Ross, Detrital zircon geochronology of Neoproterozoic to Permian miogeoclinal strata in Brit- ish Columbia and Alberta, Can. J. Earth Sci. 35 (1998) 1380-1401.

[4] T.R. Ireland, T. Fiøttman, C.M. Fanning, G.M. Gibson, W.V. Preiss, Development of the early Paleozoic Pacific margin of Gondwana from detrital-zircon ages across the Delamerian orogen, Geology 26 (1998) 243-246.

[5] J.D. Keppie, D.W. Davies, T.E. Krogh, U-Pb geochrono- logical constraints on Precambrian stratified units in the Avalon Composite Terrane of Nova Scotia, Canada: tectonic implications, Can. J. Earth Sci. 35 (1998) 222- 236.

[6] J. Fernández-Suárez, G. Gutiẽrrez Alonso, G.A. Jenner, M.N. Tubrett, New ideas on the Proterozoic-Early Paleo- zoic evolution of NW Iberia. Insights from U-Pb detrital zircon ages, Precambrian Res. 102 (2000) 185-206.

[7] K. Yamasita, R.A. Creaser, M.E. Villeneuve, Integrated Nd isotopic and U-Pb detrital zircon systematics of clastic sedimentary rocks from the Slave Province, Canada: evi- dence for extensive crustal reworking in the early- to mid- Archean, Earth Planet. Sci. Lett. 174 (2000) 283-299.

[8] J.W.F. Ketchum, S.E. Jackson, N.G. Culshaw, S.M. Barr, Depositional and tectonic setting of Paleoproterozoic Lower Aillik group, Makkovik Province, Canada: evolu- tion of a passive margin-foredeep sequence based on pet- rochemistry and U-Pb (TIMS and LAM-ICP-MS) geo- chronology, Precambrian Res. 105 (2001) 331-356.

[9] R.F. Berry, G.A. Jenner, S. Mefre, M.N. Tubrett, A North American provenance for Neoproterozoic to Cam- brian sandstones in Tasmania?, Earth Planet. Sci. Lett. 192 (2001) 207-222.

[10] J.B. Murphy, R.D. Nance, Sm-Nd isotope systematics as tectonic tracers: an example from West Avalonia in the Canadian Appalachians, Earth Sci. Rev. 1246 (2002) in press.

[11] J.B. Murphy, R.A. Strachan, R.D. Nance, K.D. Parker, M.B. Fowler, Proto-Avalonia: A 1.2-1.0 Ga tectonother- mal event and constraints for the evolution of Rodinia, Geology 28 (2000) 1071-1074.

[12] H. Kemmitz, R.L. Romer, O. Oncken, Gondwana break- up and the northern margin of the Saxothuringian belt (Variscides of Central Europe), Int. J. Earth Sci. 91 (2002) 246-259.

[13] I.W.D. Dalziel, Neoproterozoic-Paleozoic geography and tectonics: Review, hypothesis, environmental speculation, Geol. Soc. Am. Bull. 109 (1997) 16-42.

[14] J.A. Tait, V. Bachtadse, W. Franke, H.C. Sofel, Geodya- mic evolution of the European Variscan fold belt: paleo- magnetic and geological constraints, Geol. Rundschau 86 (1997) 585-598.

[15] C.McA. Powell, S.A. Pisarevsky, Late Neoproterozoic assembly of East Gondwana, Geology 30 (2002) 3-6.

[16] L. Eguiluz, J.I. Gil Ibarguchi, B. Abalos, A. Apraiz, Superposed Hercynian and Cadomian orogenic cycles in the Ossa Morena Zone and related areas of the Iberian Massif, Geol. Soc. Am. Bull. 112 (2000) 1398-1413.

[17] J. Fernández-Suárez, G. Gutiérrez Alonso, R. Cox, G.A. Jenner, Assembly of the Armorica microplate: A strike- slip terrane delivery? Evidence from U-Pb ages of detrital zircons, J. Geol. 110 (2002) 619-626.

[18] E.A. Nagy, S.D. Samson, R.S. D'Lemos, U-Pb geochro- nological constraints on the timing of Brioverian sedimen- tation and regional deformation in the St. Brieuc region of the Neoproterozoic Cadomian orogen, northern France, Precambrian Res. 116 (2002) 1-17.

[19] T.E. Jefries, S.E. Jackson, H.P. Longerich, Application of a frequency quintupled Nd:YAG source (Lamb- da = 213 nm) for laser ablation inductively coupled plas- ma mass spectrometric analysis of minerals, J. Anal. At. Spectrosc. 13 (1998) 935-940.

[20] T.E. Jefries, J. Fernández-Suárez, Zircon dating 3213nm versus 266nm Nd:YAG lasers, Application Note, New Wave Research-Merchantek Products, 2001, 2 pp.

[21] M. Wiedenbeck, P. Allẽ, F. Corfu, W.L. Griń, M. Mei- er, F. Orbeli, A. Von Quadt, J.C. Roddick, W. Spiegel, Three natural zircon standards for U-Th-Pb, Lu-Hf, trace element and REE analyses, Geostandards Newslett. 19 (1995) 1-23.

[22] T. Andersen, Correction for common-lead in U-Pb anal- yses that do not report ^{204}Pb, Chem. Geol. (2002) in press.

[23] W. Compston, I.S. Williams, C. Meyer, U-Pb geochronol- ogy of zircons from Lunar Breccia 73217 using a sensitive high-mass resolution ion microprobe, J. Geophys. Res. 89 (1984) B525-B534.

[24] W. Compston, Geological age by instrumental analysis, Mineral. Mag. 63 (1999) 297-311.

[25] B. Ordonez Casado, Geochronological studies of the Pre- Mesozoic basement of the Iberian Massif: The Ossa Mo- rena Zone and the allochthonous complexes within the Central Iberian Zone, ETH diss. 12.940 (1998) 235 pp.

[26] I. Horn, R.L. Rudnick, W.F. McDonough, Precise ele- mental and isotope ratio determination by simultaneous solution nebulization and laser ablation ICP-MS: appli- cation to U-Pb geochronology, Chem. Geol. 167 (2000) 405-425.

[27] K.R. Ludwig, On the treatment of concordant uranium- lead ages, Geochim. Cosmochim. Acta 62 (1998) 665-676.

[28] B.V. Miller, S.D. Samson, R.S. D'Lemos, U-Pb geochro- nological constraints on the timing of plutonism, volca- nism, and sedimentation, Jersey, Channel Islands, UK, J. Geol. Soc. London 158 (2001) 243-252.

[29] R.D. Nance, M.D. Thompson (Eds.), Avalonian and re- lated Peri-Gondwanan Terranes of the circum-North At- lantic, Geol. Soc. Am. Spec. Publ. 304, 1996.

[30] K.P. Hefernan, H. Admou, A.K. Jefrey, A. Saquaque, Anti-Atlas (Morocco) role in Neoproterozoic west Gond- wana reconstruction, Precambrian Res. 103 (2000) 89-96.

[31] F.F. Alkmim, S. Marshak, M.A. Fonseca, Assembling west Gondwana in the Neoproterozoic: Clues from the Sao Francisco craton region, Brazil, Geology 29 (2001) 319-322.

[32] G. Rocci, G. Bronner, M. Deschamps, Crystalline base- ment of the west African craton, in: R.D. Dallmeyer, J.P. Lecorche (Eds.), The West African Orogens and Circum- Atlantic Correlatives, Springer, Berlin, 1991, pp. 31-61.

[33] W. Teixeira, C.C.G. Tassinari, U.G. Cordani, K. Kawa- shita, A review of the geochronology of the Amazonian craton, tectonic implications, Precambrian Res. 42 (1989) 213-227.

[34] Z.S. de Souza, A. Potrel, J.M. Lafon, F.J. Althof, M.M. Pimentel, R. Dall'Agnol, C.G. de Oliveira, Nd, Pb and Sr isotopes in the Identidade Belt, an Archean greenstone belt of the Rio Maria region (Carajás Province, Brazil): implications for the Archaean geodynamic evolution of the Amazonian craton, Precambrian Res. 109 (2001) 293-315.

[35] J.Y. Calvez, P.H. Vidal, Two billion year old relicts in the Hercynian belt of western Europe, Contrib. Mineral. Pet- rol. 65 (1978) 395-399.

[36] S.D. Samson, R.S. D'Lemos, U-Pb geochronology and Sm-Nd isotopic composition of Proterozoic gneisses, Channel Islands, UK, J. Geol. Soc. London 155 (1998) 609-618.

[37] A.N. Kouamelan, C. Delor, J.J. Peucat, Geochronological evidence for reworking of Archean terranes during the early Proterozoic (2.1 Ga) in the western Côte d'Ivoire (Man Rise-West African craton, Precambrian Res. 86 (1997) 177-199.

[38] A. Potrel, J.J. Peucat, C.M. Fanning, Archean crustal evolution of the West African craton; example of the Amsaga area (Reguibat Rise); U-Pb and Sm-Nd evidence for crustal growth and recycling, Precambrian Res. 90 (1998) 107-117.

[39] D. Thieblemont, C. Delor, A. Cocherie, J.M. Lafon, J.C. Goujou, A. Balde, M. Bah, H. Sane, C.M. Fanning, A 3.5 Ga granite gneiss basement in Guinea, further evidence for early Archean accretion within the west African cra- ton, Precambrian Res. 108 (2001) 179-194.

[40] C.C.G. Tassinari, M.J.B. Macambira, Geochronological provinces in the Amazonian craton, Episodes 22 (1999) 174-182.

[41] E. Hegner, A. Kröner, Review of Nd isotopic data and xenocrystic and detrital zircon ages from the pre-Variscan basement in the eastern Bohemian Massif: speculations on palinspastic reconstructions, in: W. Franke, V. Haak, O. Oncken, D. Tanner (Eds.), Orogenic Processes: Quantification and Modelling in the Variscan Belt, Geol. Soc. Spec. Publ. 179, 2000, pp. 167-175.

[42] G. Friedl, F. Finger, N.J. McNaughton, I.R. Fietcher, Deducing the ancestry of terranes: SHRIMP evidence for South America-derived Gondwana fragments in cen- tral Europe, Geology 28 (2000) 1035-1038.

[43] D. Gebauer, I.S. Williams, W. Compston, The develop- ment of the central European continental crust since the early Archean based on conventional and ion-microprobe dating of up to 3.84 b.y. old detrital zircons, Tectonophy- sics 157 (1989) 81-96.

[44] M. Tichomirowa, H.J. Berger, E.A. Koch, B.V. Belyatski, J. Götze, U. Kempe, L. Nasdala, U. Schaltegger, Zircon ages of high-grade gneisses in the Eastern Erzgebirge (Central European Variscides) - constraints on origin of the rocks and Precambrian to Ordovician magmatic events in the Variscan foldbelt, Lithos 56 (2001) 303- 332.

[45] J.D. Keppie, J. Dostal, F. Ortega-Gutiérrez, R. Lopez, A Grenvillian arc on the margin of Amazonia: evidence from the southern Oaxacan Complex, southern Mexico, Precambrian Res. 112 (2001) 165-181.

[46] T.F. Nägler, H.J. Schäfer, D. Gebauer, Evolution of the Western European continental crust: implications from Nd and Pb isotopes in Iberian sediments, Chem. Geol. 121 (1995) 345-347.

[47] E. Mullane, The geochemistry of the South Portuguese Zone, Spain and Portugal, unpublished Ph.D. Thesis, University Southampton, UK, 1998, 260 pp.

[48] F. Paris, M. Robardet, Early Palaeozoic palaeobiogeog- raphy of the Variscan regions, Tectonophysics 177 (1990) 193-213.

[49] W.S. McKerrow, C.R. Scotese (Eds.), Palaeozoic Palaeo-geography and Biogeography, The Geological Society Memoir 12, 1990, 435 pp.

[50] J.F. Simancas, D. Martínez Poyatos, I. Expósito, A. Azor, F. González Lodeiro, The structure of a major suture zone in the SW Iberian Massif: the Ossa More- na/Central Iberian contact, Tectonophysics 332 (2001) 295-308.

[51] J.L. Bonjour, J.J. Peucat, J.J. Chauvel, F. Paris, J. Cor- nichet, U-Pb zircon dating of the Early Paleozoic (Areni- gian) transgression in western Brittany (France): a new constraint for the Lower Paleozoic time-scale, Chem. Geol. 72 (1988) 329-336.